

DOI: 10.1039/c0dt00527d

Supporting Informations

for

**An unusual (H_2O)₂₀ discrete water cluster in the supramolecular host of
a charge transfer platinum(II) complex: cytotoxicity and DNA cleavage
activities**

Sutanuva Mandal,[†] Alfonso Castiñeiras,[#] Tapan K. Mondal,[§] Arindam Mondal,[‡]
Dhrubajyoti Chattopadhyay,[‡] and Sreebrata Goswami^{†,*}

[†] Department of Inorganic Chemistry, Indian Association for the Cultivation of Science, Kolkata 700 032, India. [#]Departamento de Química Inorgánica, Universidade de Santiago de Compostela, Campus Universitario Sur, 15782 Santiago de Compostela, Spain.

[§] Department of Chemistry, Jadavpur University, Kolkata 700032, India. [‡]Dr. B. C. Guha Centre for Genetic Engineering and Biotechnology, University of Calcutta, Kolkata-700 019, India.

E-mail: icsg@iacs.res.in

Table of Contents		
	LIST OF TABLES	Page Number
Table S1	The bond distances (in Å) obtained at the B3LYP/sdd level optimized geometry [1]Cl	4
Table S2	Selected Molecular Orbitals along with their energies and compositions of compound [1]Cl in gas phase b3lyp/sdd level calculation	5
Table S3	Selected list of vertical excitations computed at the TD-DFT/B3LYP/6-31+G**//B3LYP/6-31G* level of theory for [1]Cl	6
Table S4	Selected Molecular Orbitals along with their energies and compositions of one electron reduced compound, [1] in gas phase b3lyp/sdd level calculation	7-8
Table S5	Selected list of vertical excitations computed at the TD-DFT/B3LYP/6-31+G**//B3LYP/6-31G* level of theory for one electron reduced compound, [1]	9
	LIST OF FIGURES	
Figure S1	ESI-MS spectrum of the compound [1]Cl. Inset: simulated isotopic pattern.	10
Figure S2	^1H NMR spectrum of the compound [1]Cl. in methanol-d ₄ .	11
Figure S3	Thermograms of compound [1]Cl·3.3H ₂ O showing TGA and DTA at the heating rate of 10 °C/min.	12
Figure S4	FT IR spectrum of the compound, [1]Cl·3.3H ₂ O.	13
Figure S5	Figure S5. PXRD spectra: (A) Simulated spectrum of [1]Cl·3.3 H ₂ O, (B) Experimental spectrum of [1]Cl·3.3 H ₂ O and (C) Experimental spectrum of [1]Cl.	14
Figure S6	DFT calculated frontier orbitals for the compound [1]Cl.	15
Figure S7	Theoretical and experimental UV-vis spectra of [1]Cl in 10 ⁻⁴ M acetonitrile solution.	15

Figure S8	Cyclic voltammogram of the compound [1]Cl in CH ₃ CN / 0.1 M Et ₄ NClO ₄ .	16
Figure S9	DFT calculated frontier orbitals for the one electron reduced compound [1].	17
Figure S10	EPR Spectrum of electrogenerated 1 in CH ₃ CN/0.1 M Et ₄ NClO ₄ at 120K.	17
Figure S11	Emission spectra of DNA bound EtBr with increasing concentration of [1]Cl.	18
Figure S12	DNA melting curves at 260 nm in absence (□) and presence (▲) of [1]Cl.	19
Figure S13	CD spectra of uncomplexed [1]Cl (violet), free CT DNA (black), and CT DNA in the presence of [1]Cl at <i>r</i> = 20(green), 10(red), 5 (blue), in Tris-HCl, 50 mM NaCl buffer.	20
Figure S14	Effect of increasing amount of [1]Cl on the relative viscosity of CT DNA in Tris-HCl, 50 mM NaCl buffer.	21

Table S1. The bond distances (in Å) obtained at the B3LYP/sdd level optimized geometry [1]Cl

	Experimental	Theoretical
Pt(1)-S(1)	2.261(12)	2.320
Pt(1)-N(3)	1.969(4)	1.988
Pt(1)-N(1)	2.042(4)	2.076
Pt(1)-N(2)	2.020(4)	2.062
C(6)-N(2)	1.292(7)	1.306
S(1)-C(19)	1.772(5)	1.776
N(3)-C(14)	1.359(6)	1.373
S(1)-C(20)	1.824(5)	1.831
S(1)-Pt(1)-N(3)	84.37(12)	82.69
S(1)-Pt(1)-N(1)	174.7(11)	176.9
S(1)-Pt(1)-N(2)	99.02(11)	100.2
N(3)-Pt(1)-N(1)	97.76(16)	98.24
N(3)-Pt(1)-N(2)	174.4(16)	175.9
N(1)-Pt(1)-N(2)	79.25(16)	78.79
Pt(1)-S(1)-C(19)	99.51(15)	99.38
Pt(1)-N(3)-C(14)	121.4(3)	122.9
Pt(1)-N(1)-C(5)	113.7(4)	113.6
Pt(1)-N(2)-C(6)	115.4(3)	114.6
Pt(1)-N(2)-C(7)	124.6(3)	126.4

Table S2. Selected Molecular Orbitals along with their energies and compositions of compound [1]Cl in gas phase b3lyp/sdd level calculation

MO	Energy, eV	Composition		
		Pt	L ¹	(L ²) ⁻
LUMO+5	-3.18	05	89	06
LUMO+4	-3.28	07	91	02
LUMO+3	-3.37	16	13	71
LUMO+2	-4.44	44	24	32
LUMO+1	-4.61	03	96	01
LUMO	-6.00	07	86	07
HOMO	-7.80	08	09	83
HOMO-1	-9.38	02	02	96
HOMO-2	-9.45	03	94	03
HOMO-3	-9.94	08	87	05
HOMO-4	-10.03	63	17	20
HOMO-5	-10.07	60	10	30
HOMO-6	-10.46	63	17	20
HOMO-7	-11.08	07	70	23
HOMO-8	-11.18	34	22	44
HOMO-9	-11.66	50	18	32
HOMO-10	-11.70	30	19	51
HOMO - LUMO = 1.80 eV				

Table S3. Selected list of vertical excitations computed at the TD-DFT/B3LYP/6-31+G**//B3LYP/6-31G* level of theory for [1]Cl

Excited State	Wavelength (nm)	f	Energy (eV)	Transition	Character	Experimental (λ , nm)
1	672.7	0.156	1.843	(86%)HOMO → LUMO	$[(L^2)](\pi) \rightarrow L^1(\pi^*)$, ILCT	642
3	413.2	0.023	3.000	(73%)HOMO-3 → LUMO	$L^1(\pi) \rightarrow L^1(\pi^*)$, ILCT	
5	395.1	0.196	3.138	(82%)HOMO-1 → LUMO	$[(L^2)](\pi) \rightarrow L^1(\pi^*)$, ILCT	338
6	372.9	0.046	3.325	(77%)HOMO-2 → LUMO	$L^1(\pi) \rightarrow L^1(\pi^*)$, ILCT	
8	344.0	0.038	3.604	(67%)HOMO-5 → LUMO	Pt(d π) → $L^1(\pi^*)$, MLCT	
10	325.5	0.077	3.809	(66%)HOMO-6 → LUMO	Pt(d π) → $L^1(\pi^*)$, MLCT	
16	278.3	0.087	4.454	(71%)HOMO → LUMO+5	$[(L^2)](\pi) \rightarrow L^1(\pi^*)$, ILCT	
19	269.9	0.040	4.593	(41%)HOMO-7 → LUMO (22%)HOMO-1 → LUMO+2	$L^1(\pi) \rightarrow L^1(\pi^*)$, ILCT $[(L^2)](\pi) \rightarrow Pt(d\pi)$, LMCT	
21	264.06	0.113	4.684	(26%)HOMO-3 → LUMO+2 (24%)HOMO-1 → LUMO+2	$L^1(\pi) \rightarrow Pt(d\pi)$, LMCT $[(L^2)](\pi) \rightarrow Pt(d\pi)$, LMCT	284
22	262.8	0.065	4.717	(43%)HOMO-3 → LUMO+2 (27%)HOMO-1 → LUMO+2	$L^1(\pi) \rightarrow Pt(d\pi)$, LMCT $[(L^2)](\pi) \rightarrow Pt(d\pi)$, LMCT	

Table S4. Selected Molecular Orbitals along with their energies and compositions of one electron reduced compound [1] in gas phase b3lyp/sdd level calculation

α -MO				
MO	Energy	Composition		
		Pt	L ¹	[L ²] ⁻
LUMO+5	0.30	49	43	08
LUMO+4	0.15	45	41	14
LUMO+3	-0.15	14	83	03
LUMO+2	-0.37	11	12	77
LUMO+1	-0.73	04	91	05
LUMO	-0.78	44	28	28
HOMO	-3.58	08	85	07
HOMO-1	-4.67	11	11	78
HOMO-2	-6.04	13	79	08
HOMO-3	-6.25	93	03	04
HOMO-4	-6.44	20	15	65
HOMO-5	-6.72	34	31	35
HOMO-6	-6.81	39	33	28
HOMO-7	-6.83	18	77	05
HOMO-8	-7.45	14	73	13
HOMO-9	-7.62	55	19	26
HOMO-10	-8.09	23	33	44

β -MO				
MO	Energy	Composition		
		$[(L^2)^-]$	L ¹	Pt
LUMO+5	0.18	16	26	58
LUMO+4	-0.11	03	81	16
LUMO+3	-0.33	68	23	09
LUMO+2	-0.57	14	81	05
LUMO+1	-0.72	28	28	44
LUMO	-1.90	04	89	07
HOMO	-4.56	79	07	14
HOMO-1	-5.76	09	81	10
HOMO-2	-6.22	04	03	93
HOMO-3	-6.41	57	18	25
HOMO-4	-6.64	26	36	38
HOMO-5	-6.70	38	25	37
HOMO-6	-6.78	07	92	01
HOMO-7	-7.13	12	72	16
HOMO-8	-7.58	31	11	58
HOMO-9	-7.98	27	48	25
HOMO-10	-8.23	21	56	23

Table S5. Selected list of vertical excitations computed at the TD-DFT/B3LYP/6-31+G**//B3LYP/6-31G* level of theory for one electron reduced compound, [1]

Excited State	Wavelength (nm)	f	Energy (eV)	Transition	Character	Experimental (λ , nm)
2	668.1	0.0214	1.8558	(90%)HOMO(α) → LUMO+1(α)	$L^1(\pi) \rightarrow L^1(\pi^*)$, ILCT	560
3	596.5	0.0676	2.0787	(92%)HOMO(β) → LUMO(β)	$[(L^2)^-](\pi) \rightarrow L^1(\pi^*)$, ILCT	
10	480.4	0.1156	2.5808	(53%)HOMO(α) → LUMO+4(α)	$L^1(\pi) \rightarrow L^1(\pi^*)/ Pt(d\pi)$, ILCT, LMCT	
11	373.0	0.1373	3.3240	(50%)HOMO(α) → LUMO+5(α) (28%)HOMO(α) → LUMO+6(α)	$L^1(\pi) \rightarrow L^1(\pi^*)/ [(L^2)^-](\pi^*)/ Pt(d\pi)$, ILCT, LMCT	364
20	307.3	0.1422	4.0346	(51%)HOMO-3(β) → LUMO(β)	$[(L^2)^-](\pi)/ L^1(\pi) \rightarrow L^1(\pi^*)$, ILCT	298

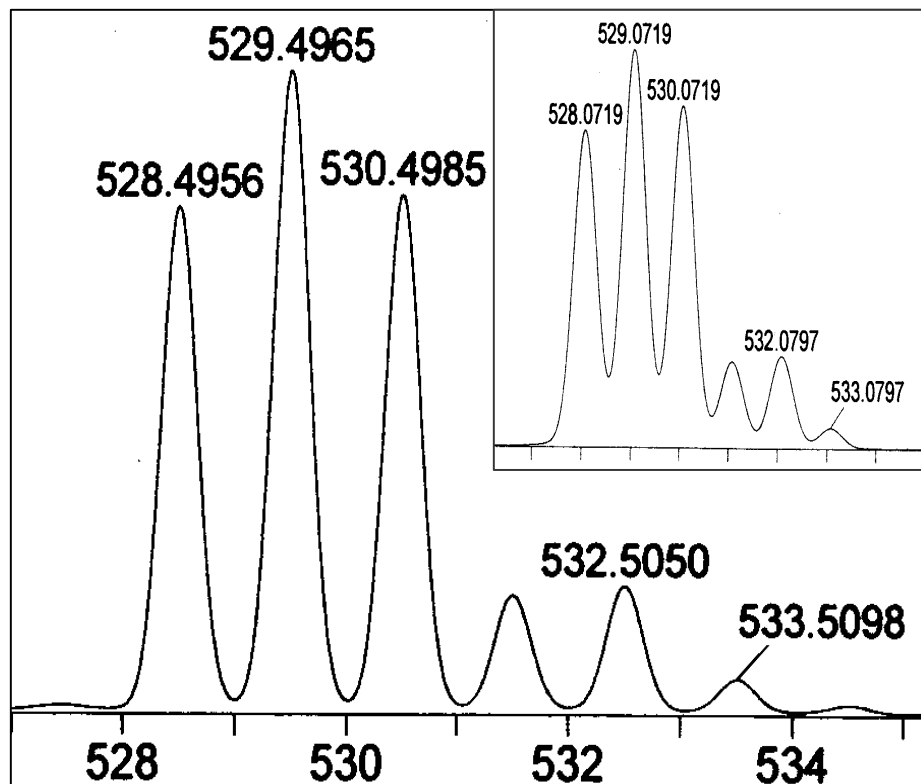


Figure S1. ESI-MS spectrum of the compound [1]Cl. Inset: simulated isotopic pattern.

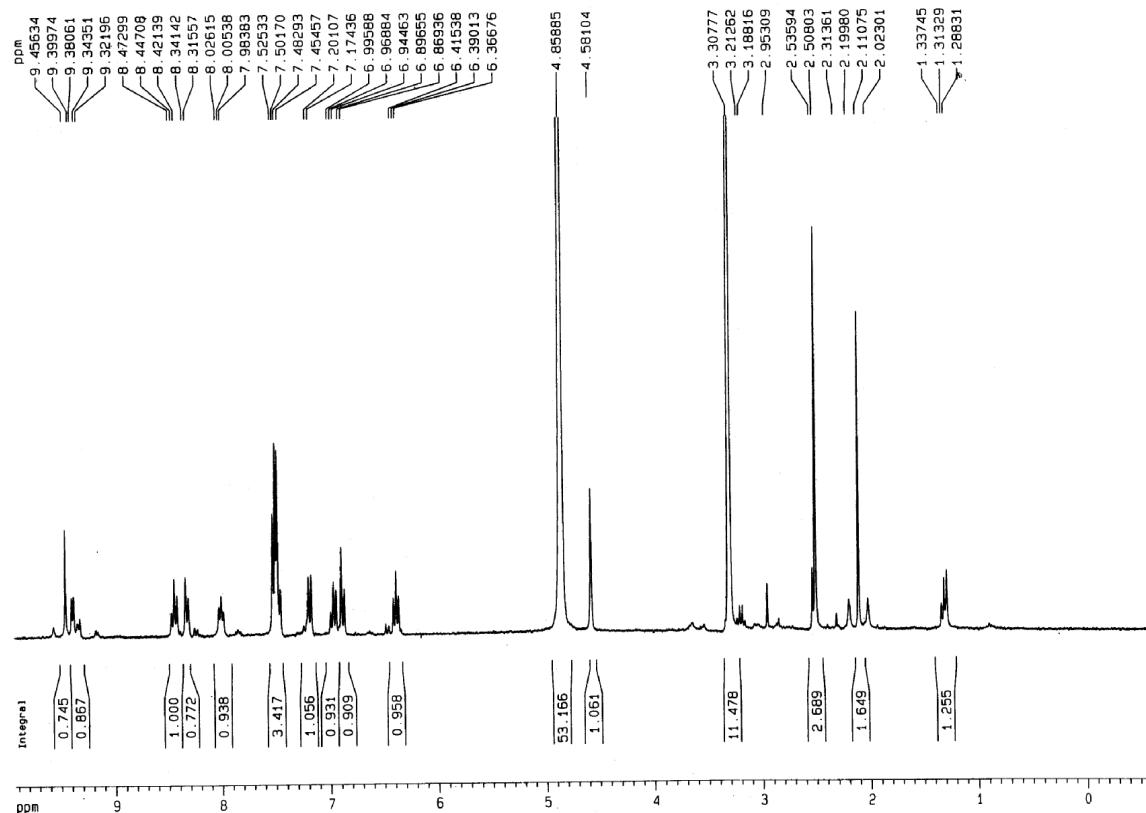


Figure S2. ^1H NMR spectrum of the compound [1]Cl in methanol-d₄.

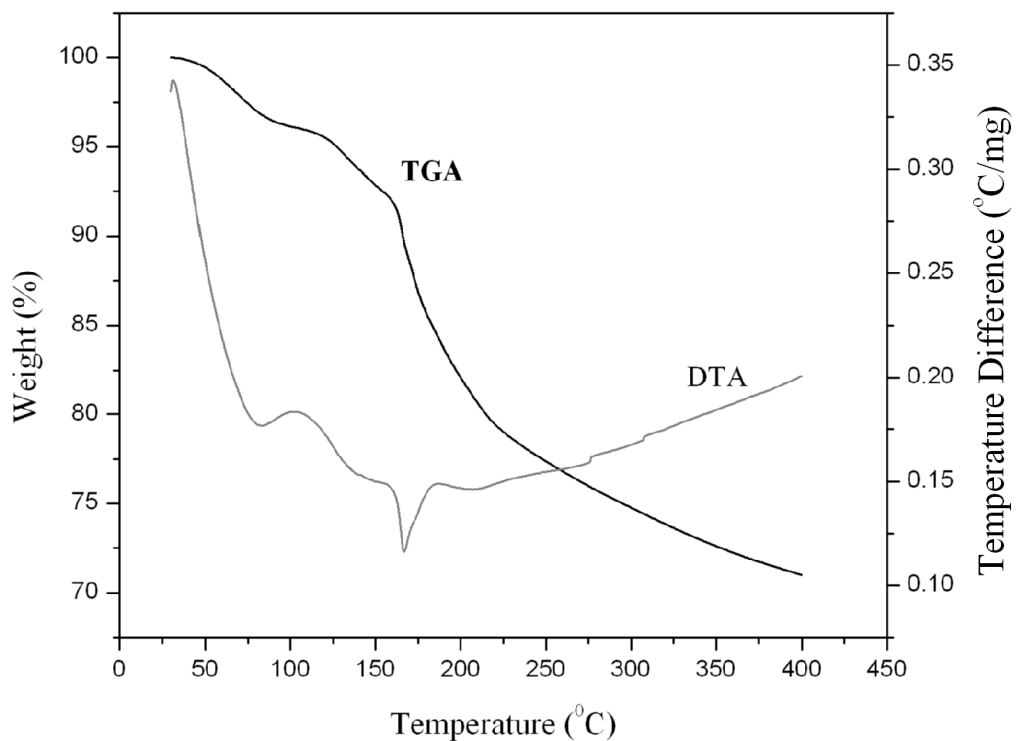


Figure S3. Thermograms of compound **[1]**Cl·3.3H₂O showing TGA (black) and DTA (grey) at the heating rate of 10 °C/min.

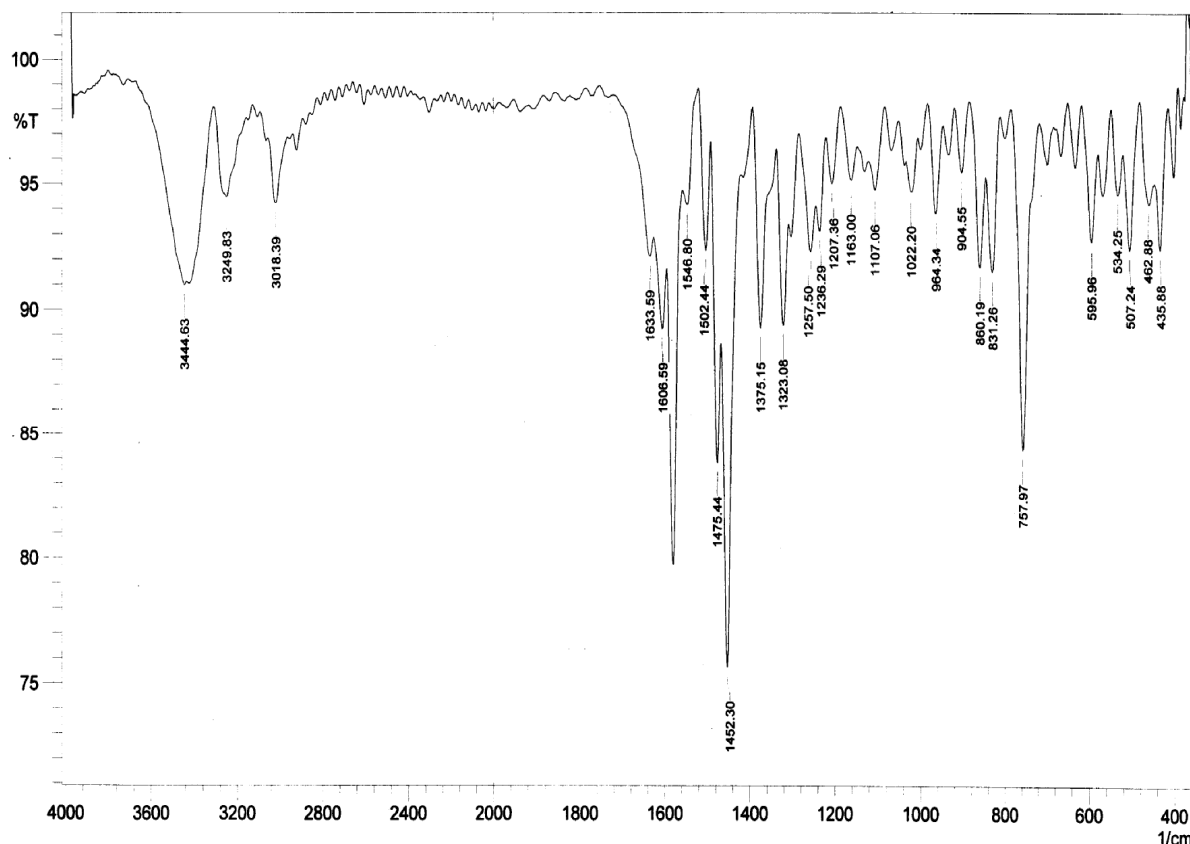


Figure S4. FT IR spectrum of the compound $[1]\text{Cl}\cdot3.3\text{H}_2\text{O}$.

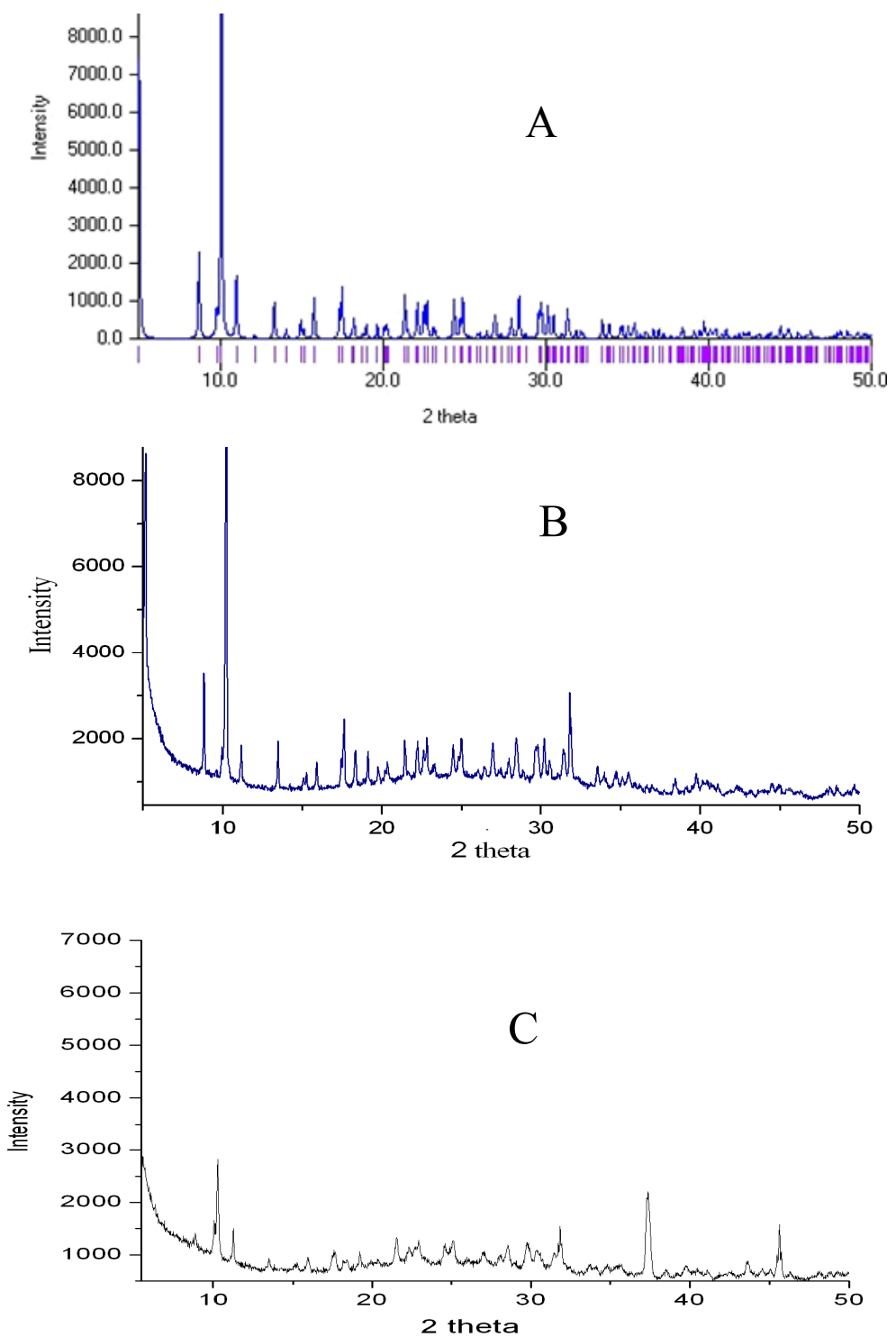


Figure S5. PXRD spectra: (A) Simulated spectrum of $\mathbf{[1]Cl \cdot 3.3 H_2O}$, (B) Experimental spectrum of $\mathbf{[1]Cl \cdot 3.3 H_2O}$ and (C) Experimental spectrum of $\mathbf{[1]Cl}$.

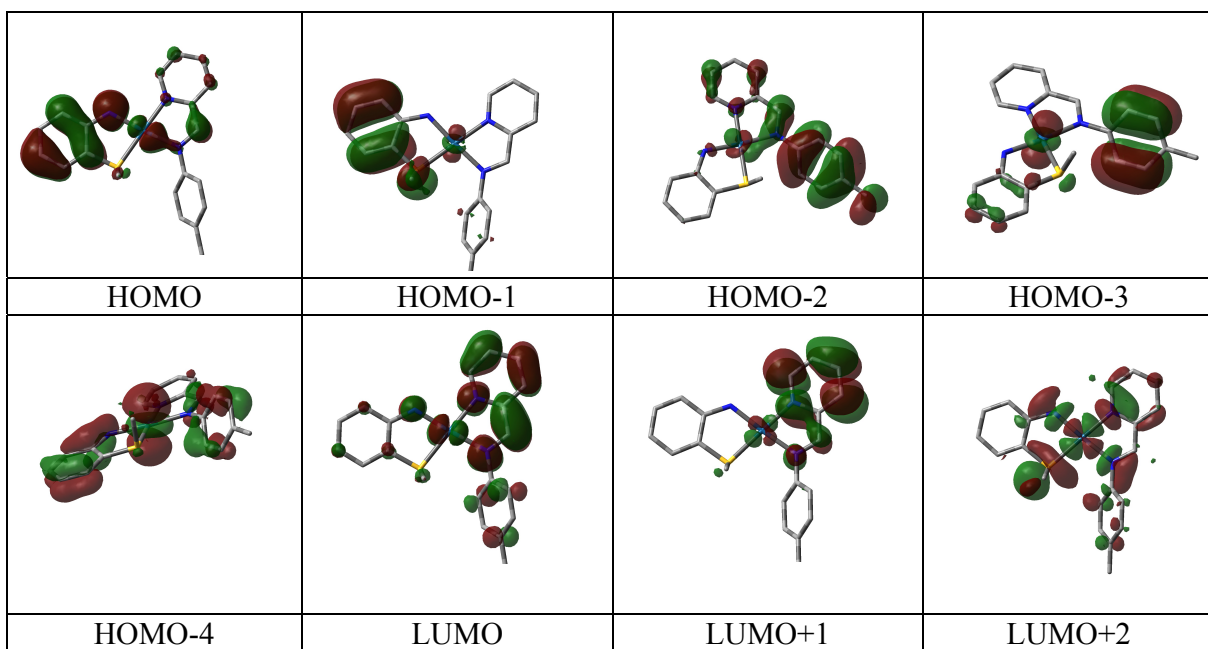


Figure S6. DFT calculated frontier orbitals for the compound [1]Cl.

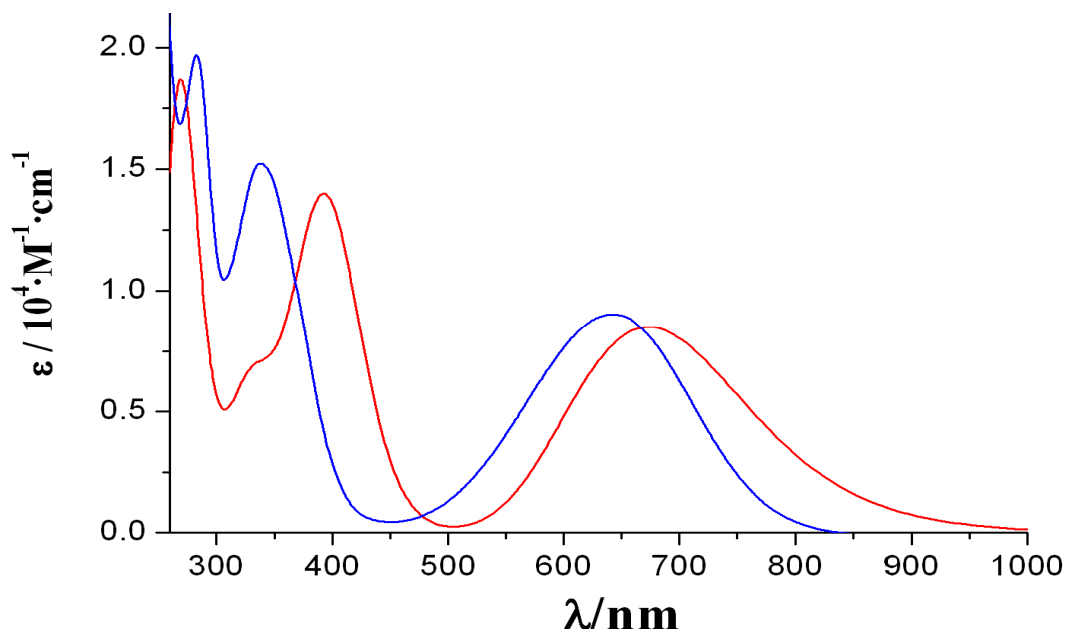


Figure S7. Theoretical and experimental UV-vis spectra of [1]Cl in 10^{-4} M acetonitrile solution. Colour code: blue (experimental), red (theoretical).

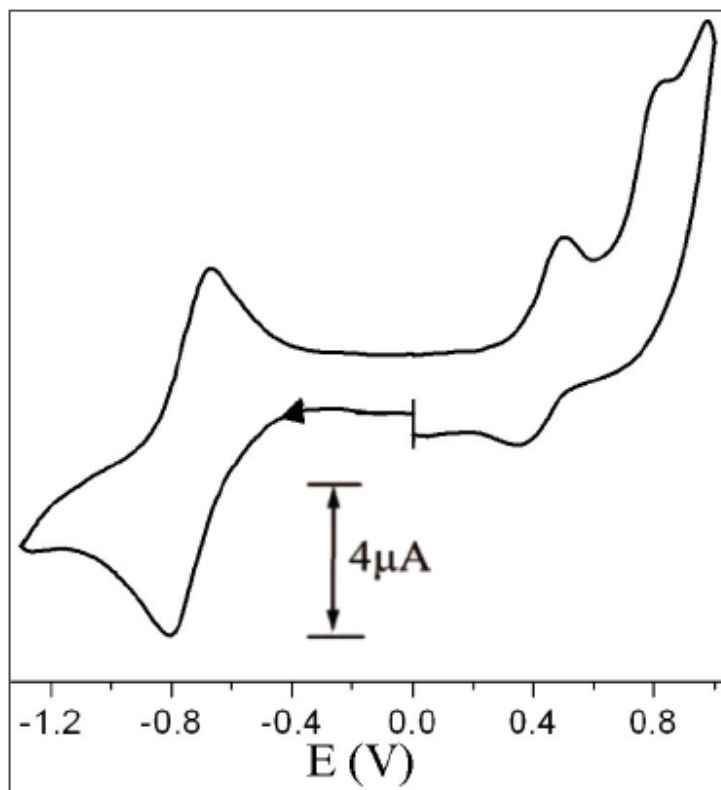


Figure S8. Cyclic voltammogram of the compound $[1]\text{Cl}$ in $\text{CH}_3\text{CN} / 0.1 \text{ M Et}_4\text{NClO}_4$.

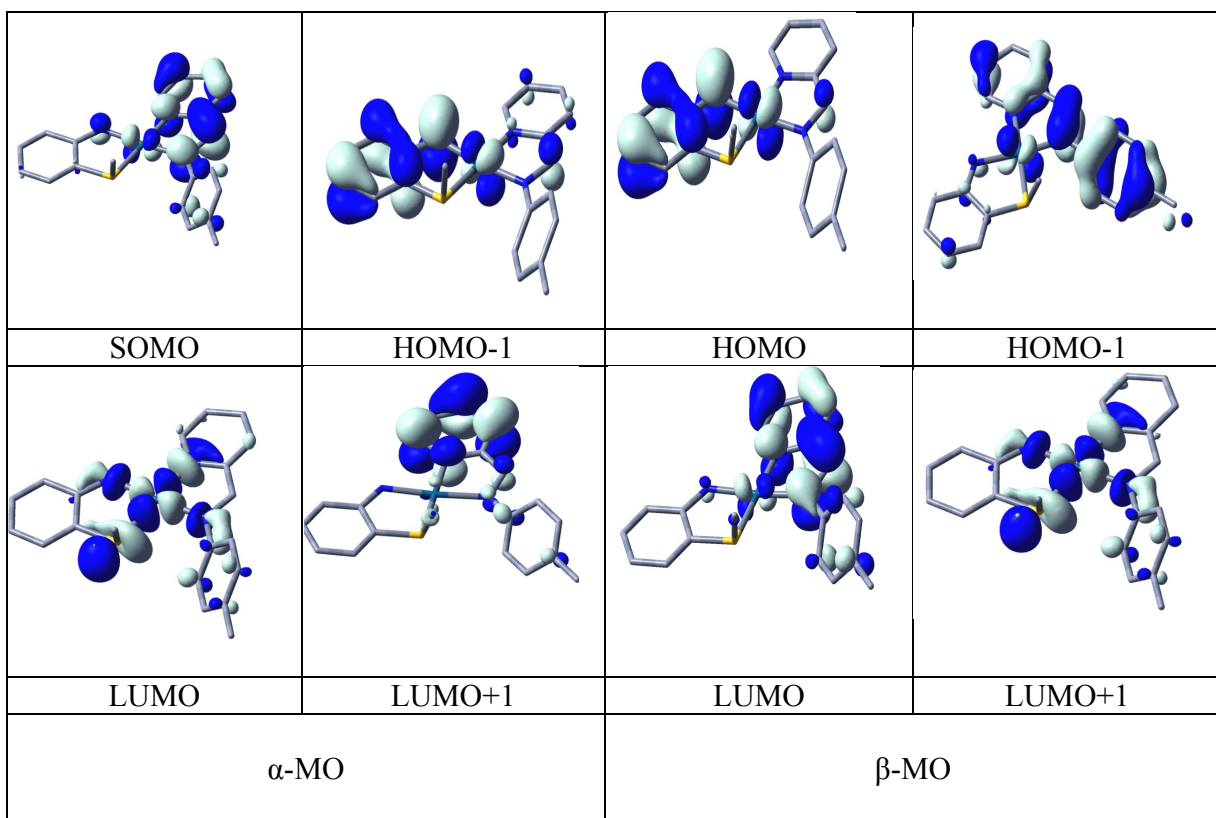


Figure S9. DFT calculated frontier orbitals for the one electron reduced compound **[1]**.

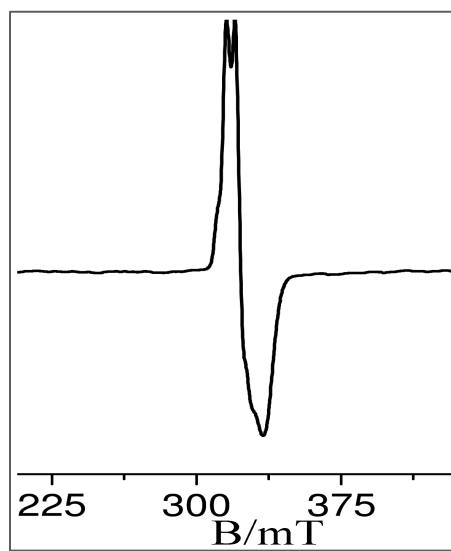


Figure S10. EPR Spectrum of electrogenerated **1** in $\text{CH}_3\text{CN}/0.1 \text{ M Et}_4\text{NClO}_4$ at 120K.

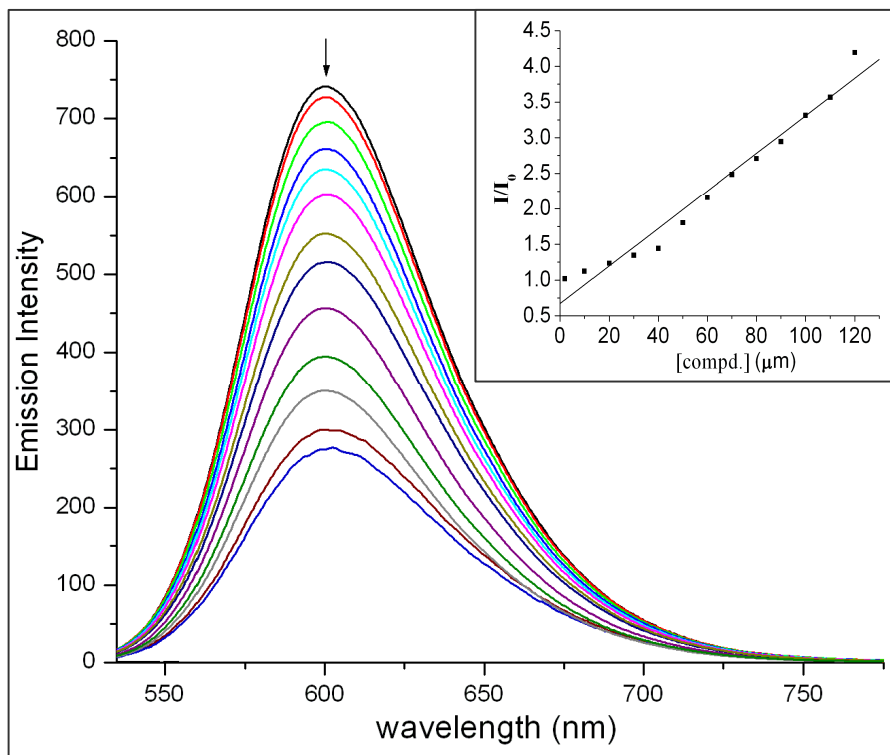


Figure S11. Emission spectra of DNA bound EtBr with increasing concentration of **[1]Cl**.

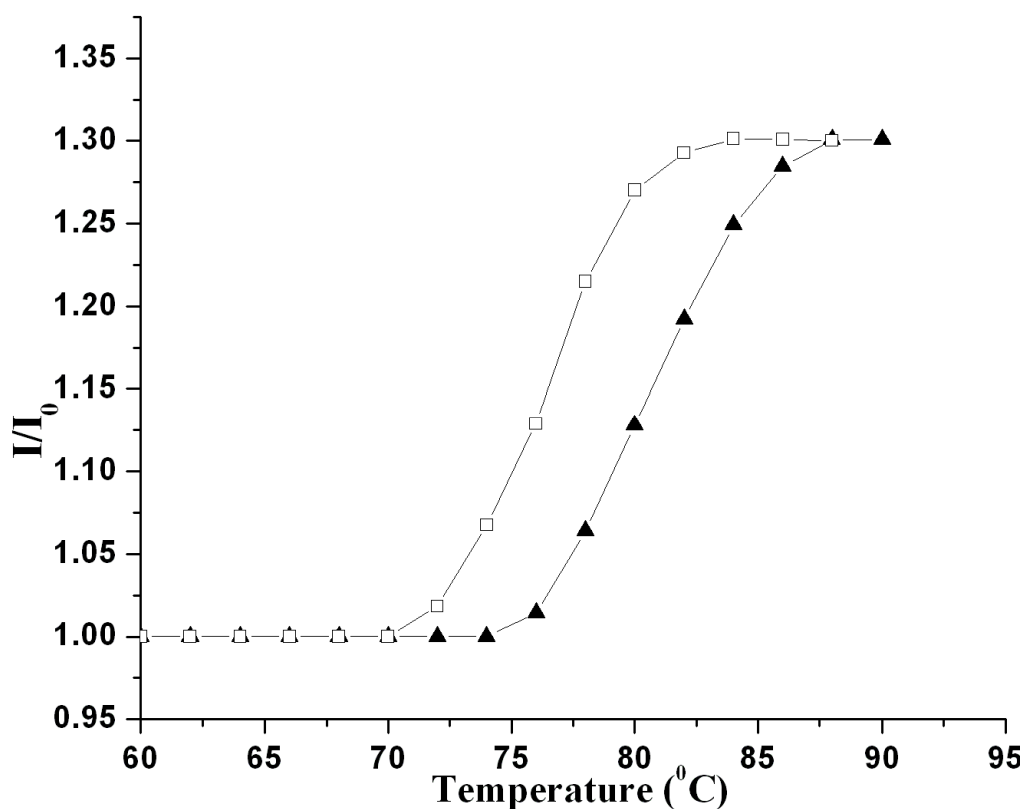


Figure S12. DNA melting curves at 260 nm in absence (□) and presence (▲) of [1]Cl.

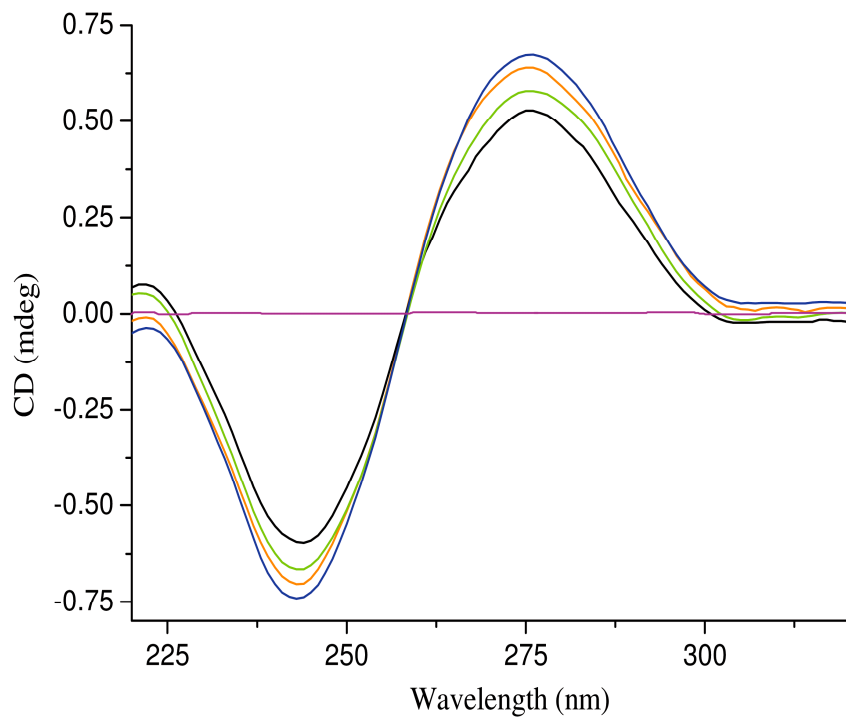


Figure S13. CD spectra of uncomplexed **[1]**Cl (violet), free CT DNA (black), and CT DNA in the presence of **[1]**Cl at $r = 20$ (green), 10(red), 5 (blue), in Tris-HCl, 50 mM NaCl buffer.

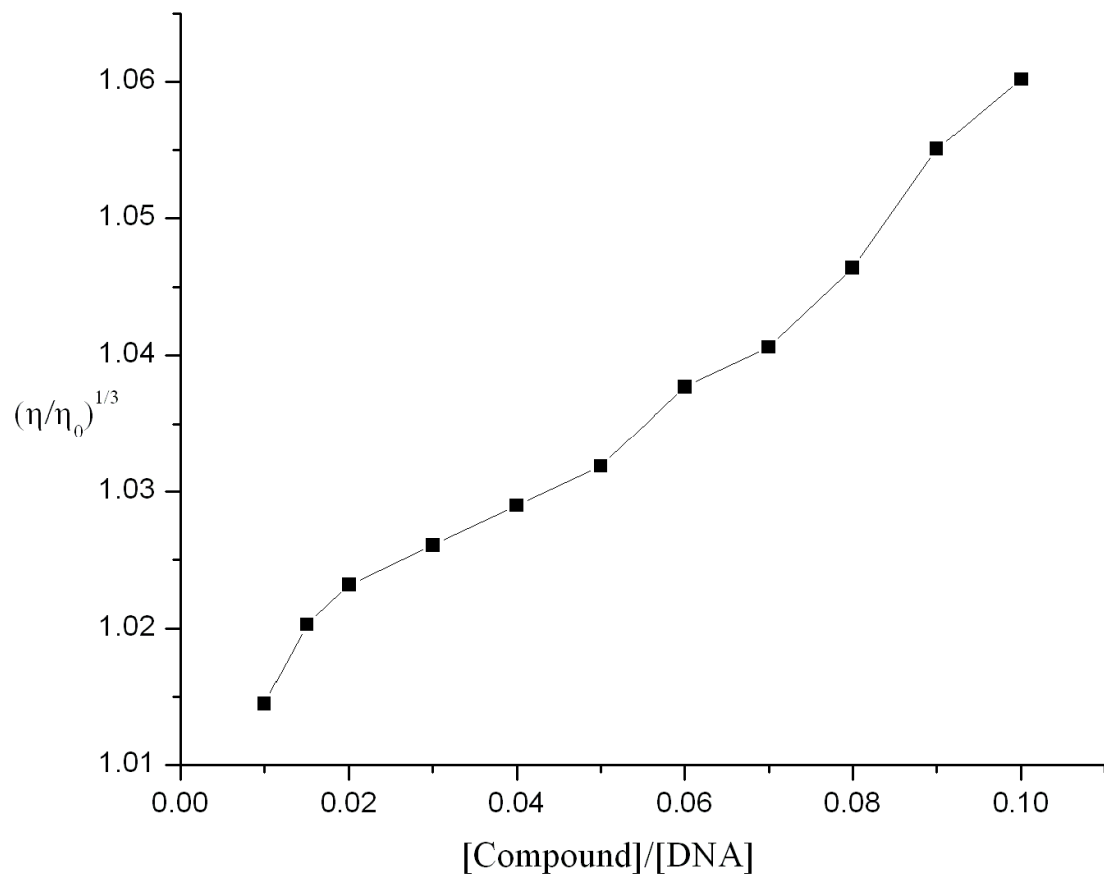


Figure S14. Effect of increasing amount of **[1]Cl** on the relative viscosity of CT DNA in Tris-HCl, 50 mM NaCl buffer.